



---

*Research article*

## An investigative study on the parameters optimization of the electric discharge machining of Ti6Al4V

Muhammad Mansoor Uz Zaman Siddiqui<sup>1,2,\*</sup>, Syed Amir Iqbal<sup>1</sup>, Ali Zulqarnain<sup>1</sup> and Adeel Tabassum<sup>2,3</sup>

<sup>1</sup> Department of Industrial & Manufacturing Engineering, NED University of Engineering & Technology, Karachi-75270, Pakistan

<sup>2</sup> Quality Department, PEL, 14 km Ferozepur Road, Lahore-54600, Pakistan

<sup>3</sup> Department of Mechanical Engineering, NUST College of EME, Rawalpindi, Pakistan

\* **Correspondence:** Email: mansoorresearch1986@gmail.com.

**Abstract:** This investigative study explored the field of electrical discharge machining (EDM), with a particular focus on the machining of Ti6Al4V, a titanium alloy that finds widespread application in aerospace, airframes, engine components, and non-aerospace applications such as power generation and marine and offshore environments. Ti6Al4V presents difficulties for conventional metal cutting techniques because of high cutting forces, poor surface integrity, and tool wear. This has led to the adoption of unconventional techniques like EDM. However, problems like high electrode wear rates, low material removal rates, long machining times, and less-than-ideal surface finishes still exist, especially in large-scale applications. By addressing the particular difficulties associated with large-scale electrical discharge machining and by putting forth a multi-objective optimization strategy, this research makes a substantial contribution to the field. With an emphasis on the optimization of input parameters like pulse on time ( $T_{on}$ ), pulse off time ( $T_{off}$ ), voltage (HV), and current (LV), which are critical in large-scale industrial applications, the study attempts to evaluate the optimal parameter states that simultaneously accomplish multiple goals during the machining process. This work is the first to simultaneously optimize all relevant output responses, such as material removal rate (MRR), electrode wear rate (EWR), machining time ( $T_m$ ), surface roughness ( $R_a$ ), and base radius. Previous studies have concentrated on one or two output responses. To optimize MRR, EWR,  $T_m$ ,  $R_a$ , and base radius, the experiments were carefully planned using design of experiment (DOE) and response Surface methodology (RSM). Regression analysis and ANOVA are two statistical techniques that were used with Minitab 15 to help interpret experimental data and build a solid regression model specifically

for Ti6Al4V. Throughout the experiment, a variety of input factor settings were employed, and the responses to those were noted. The following parameters were used to obtain the experimental data: current (LV) at 30 and 50 A, voltage (HV) at 0.3 and 0.7 V, pulse on time ( $T_{on}$ ) at 4 and 6.5  $\mu$ s, and pulse off time ( $T_{off}$ ) at 5.5 and 6.5  $\mu$ s.  $T_{on}$  and current are the most significant variables that influence most of the output responses. By addressing the simultaneous optimization of multiple output responses, this investigative study not only sets a new standard in the field but also identifies current bottlenecks and offers solutions.

**Keywords:** electric discharge machining; material removal rate; electrode wear rate; surface roughness; machining time; Ti6Al4V; design of experiment; analysis of variance

---

**Abbreviations and symbols:** ANOVA: Analysis of variance; Doc: Depth of cut; EDM: Electric discharge machining; MRR: Material removal rate; EWR: Electrode wear rate; Ra: Surface roughness;  $T_m$ : Machining time; R: Base radius;  $T_{off}$ : Pulse off time;  $T_{on}$ : Pulse on time;  $W_a$ : Weight of workpiece after machining;  $W_b$ : Weight of workpiece before machining;  $E_a$ : Weight of electrode after machining;  $E_b$ : Weight of electrode before machining

## 1. Introduction

There are two types of machining techniques; conventional and non-conventional. In conventional machining, material is removed from a workpiece by cutting, shearing, or abrasion using mechanical techniques like turning, milling, drilling, and grinding [1]. For these techniques, the workpiece is shaped to the required size and surface smoothness using hard tools. On the contrary, non-conventional machining methods that use unusual energy sources or procedures to remove material include electrochemical machining (ECM) [2], electrical discharge machining (EDM) [3], laser cutting [4], and ultrasonic machining [5]. Complex shapes, hard materials, or situations where traditional procedures are difficult or ineffective are common applications for these non-conventional machining techniques. Non-conventional machining offers greater accuracy, flexibility, and ability to work with exotic materials as compared to conventional machining techniques.

Materials with outstanding mechanical capabilities, resistance to corrosion, and less weight are always in demand by the aerospace, automotive, and biomedical industries. The titanium alloy Ti6Al4V is one of the most commonly utilized materials in these industries because of its exceptional strength, low density, and superior corrosion resistance [6]. However, because of its great strength and limited heat conductivity, this alloy is very difficult to machine. Electric discharge machining has emerged as a promising solution for Ti6Al4V machining, offering higher precision, ability to work with complex geometries, and higher productivity, which is a critical factor in aerospace and biomedical industries that work under very strict schedules for on time deliveries [7]. Ti-6Al-4V is a Grade-5 alloy of titanium and is known as the “workhorse” of the titanium alloys. It is the most commonly used of all titanium alloys. It accounts for 50% of the total titanium usage in the whole world. Its usability lies in its many benefits. Ti6Al-4V can be heat treated to increase its strength. It can be used in welded construction at service temperatures of up to 600 °F. This alloy offers its high strength with low weight, useful formability, and high corrosion resistance. Ti6Al4V’s usability makes it the best alloy for use in several industries, like the aerospace, medical, marine, and chemical processing industries. It can be

used in the creation of such technical things as aircraft turbines, engine components, aircraft structural components, aerospace fasteners, high-performance automatic parts, marine applications, sports equipment, etc. In order to improve the dimensional accuracy, surface quality, and machining efficiency of Ti6Al4V components, this study investigates the parametric optimization of EDM.

Ti6Al4V is the most widely used titanium alloy, and its uses span many aerospace, airframe, and engine component uses [8] and also major non-aerospace applications in the marine, offshore, and power generation industries in particular. Ti6Al4V is bio-compatible, and this makes it a preferred material for bio-implants like bone plates, dental implants, etc. Despite its extensive utilization in aerospace, biomedical, and automotive industries, machining Ti6Al4V using conventional methods poses significant challenges because of high cutting forces, poor surface integrity, and tool wear [9]. Despite EDM being an excellent alternative as a non-conventional machining technique for Ti6Al4V, it presents its own set of challenges. One of the major challenges that is being faced in the industry is the achievement of desired material removal rate (MRR) while maintaining excellent surface roughness, dimensional accuracy, reduced electrode wear rate, reduced machining time for higher productivity, and optimum base radius [10]. Because of the aforementioned issues, parametric optimization in EDM has become extremely crucial.

EDM is a non-conventional machining technique, and it is used to machine materials that are difficult to cut like Ti6Al4V. It has become a widely accepted technique as it can machine complex geometries in materials like Ti6Al4V that are challenging to cut [11]. EDM works on the basis of thermal erosion, which is the removal of material by localized melting and vaporization caused by regulated electrical discharges between an electrode and the workpiece. EDM, in contrast to traditional machining techniques, allows for very precise cutting of delicate features because it does not rely on mechanical contact between the tool and the workpiece, which poses its unique advantages and disadvantages [12]. A dielectric fluid separates the two electrodes, the workpiece, and the wire tool and creates an electrical circuit between them. An electrical voltage is introduced between the workpiece and the wire, causing recurrent sparks to occur [13]. The material is removed with a series of isolated electrical discharges that produce localized temperatures hot enough to melt or evaporate the metal of the workpiece.

Since the inception of in the late 1940s, there has been great advancement in the field of electric discharge machining because of development of new technologies. EDM has advanced significantly in terms of equipment development, parametric optimization, and overall efficiency from its basic origins to 2024 [14]. Within the field of equipment development, contemporary EDM machines represent the pinnacle of technological innovation. The accuracy and speed of the machining process have been completely transformed by improved control systems and servo mechanisms. These developments raise the bar for EDM operations' quality and efficiency by enabling faster cutting rates, tighter tolerances, and finer surface finishes. Chemical developments have also resulted in the creation of dielectric fluids with improved characteristics, including increased heat stability, increased flash points, increased dielectric strength, and decreased viscosity [15]. These enhancements lower the possibility of thermal damage to the workpiece, boost machining efficiency and preserve stable machining conditions.

The incorporation of advanced monitoring and feedback technologies into EDM has transformed how operators control and optimize the machining process. These systems give real-time information about essential machining parameters, enabling the early detection of deviations or abnormalities that could jeopardize process stability and product quality [16]. Sensors positioned strategically within the

EDM machine are an important component of modern monitoring systems. These sensors constantly monitor factors like discharge current, gap voltage, electrode wear rate, dielectric fluid temperature, and workpiece surface condition. The data acquired by these sensors is then transferred to a central control unit and examined in real time by multiple algorithms [17]. By monitoring these data in real time, operators can quickly detect deviations from the ideal machining conditions. For example, if the discharge current exceeds specified criteria or the electrode wear rate exceeds acceptable limits, the monitoring system can notify operators to take appropriate action [18]. Furthermore, advanced monitoring systems are frequently integrated with predictive analytics capabilities, which allow them to anticipate potential problems before they arise. By examining past data and patterns, these systems can forecast when certain components will break or when machining conditions will become unstable. This proactive strategy allows operators to anticipate future faults, reducing downtime and assuring continuous output.

Researchers and manufacturers are constantly addressing and improving many elements of EDM. Surface finish, which is especially important in industries like aerospace and biomedical engineering, can be jeopardized by issues such as recast layer development, micro-cracking, and surface roughness [8,19,20]. Another major difficulty in EDM is electrode wear rate, which causes dimensional inaccuracies, decreased efficiency, and increased tooling costs. EDM often operates at a slower rate than traditional processes such as milling or turning, particularly when working with complex geometries or large material volumes. Balancing efficiency, precision, and surface quality is a significant problem, highlighting the need for optimizing material removal rate and machining time. Researchers frequently focus on optimizing one or two output factors at a time, making it difficult for manufacturers to make changes to input parameters while optimizing all essential output parameters efficiently [21,22].

In large-scale industrial applications, the paramount significance lies in optimizing input parameters such as pulse on time ( $T_{on}$ ), pulse off time ( $T_{off}$ ), voltage (HV), and current (LV). These input variables play a pivotal role as they directly influence various output responses, including MRR, electrode wear rate (EWR), machining time ( $T_m$ ), surface roughness (Ra), and base radius. While existing studies focus on optimizing one or two output responses concurrently, no current research has been conducted to date to optimize all of the output responses simultaneously and efficiently [23]. In this research study, five output responses were to be optimized simultaneously. This parametric optimization was performed in a controlled environment with lower ranges of input factors, and still positive results were observed.

## 2. Materials and methods

### 2.1. Materials

The selection of Ti6Al4V is based on its position as the most widely used titanium alloy with a wide range of applications across multiple industries. Ti6Al4V was procured from Xi'an JoinXin New Material Technology Co., Ltd. The decision to use copper as an electrode was because copper continues to outperform graphite in finishing technologies in terms of obtaining a desired surface quality. When using a graphite electrode, increased tool wear and poor surface quality are observed [24]. Kerosene oil was used as a dielectric during this experiment. Ramanuj Kumar et al. (2018) conducted a study for optimizing MRR and Ra for Ti6Al4V. The study concluded that the optimized values for

input factors were current = 18 A,  $T_{on} = 100 \mu s$ , and voltage = 40 V. The corresponding output responses were found to be  $MRR = 0.056 \text{ g/min}$ . Additionally, it was noted that  $Ra$  tends to be higher when input values are elevated and lower when input values are decreased [25].

This testing has been conducted in a controlled environment with lower ranges of input factors, yet we continue to observe positive results. These results will be discussed in detail in the results section.

### 2.1.1. Titanium alloy (Ti-6Al-4V)

The physical properties of Ti-6Al-4V [26] are presented in Table 1.

**Table 1.** Physical properties of titanium Ti6Al4V.

Quantity	Value
Density	4420 kg/m <sup>3</sup>
Hardness	326 BHN/36 HRC
Percentage elongation	10%
Percentage reduction	20%
Tensile strength	1000 MPa
Yield strength	910 MPa
Young's modulus	110 GPa
Endurance limit	492 MPa
Melting point	1649 ± 15 °C
Thermal conductivity	7.2 W/Mk
Specific heat (J/(kg·°C))	560
Beta transus	999 ± 15 °C
Electrical resistivity	171 μΩ·cm @ 68 °F

### 2.1.2. Copper

Copper became the metallic electrode material of choice with the development of the transistorized, pulse-type power supplies, electrolytic (or pure). This is because the combination of copper and certain power supply settings enables low-wear burning, while in the case of graphite, high tool wear was observed. Also, copper is compatible with the polishing circuits of certain advanced power supplies. Due to its structural integrity, copper can produce very fine surface finishes as compared to graphite, even without special polishing circuits. This same structural integrity also makes copper electrodes highly resistant to DC arcing in poor flushing situations.

Copper is frequently used to make female electrodes on a wire EDM for subsequent use in reverse burning punches and cores in the sinker EDM [25]. Physical properties of copper [27] are mentioned in Table 2.

**Table 2.** Physical properties of copper.

Quantity	Value
Density	7764 kg/m <sup>3</sup>
Hardness	50 HRV
Percentage elongation	60%
Tensile strength	210 MPa
Yield strength	33.3 MPa
Modulus of elasticity	110 GPa
Bulk modulus	140 GPa
Melting point	1083 °C
Thermal conductivity	398 W/mK
Specific heat (J/(kg·°C))	385
Electrical resistivity	0.00170 μΩ·cm

## 2.2. Methods

The experiments were planned using DOE (design of experiment) and RSM (response surface methodology) for optimizing MRR, EWR, T<sub>m</sub>, Ra, and base radius.

### 2.2.1. DOE

Planning any data collection activities in the face of variability, whether or not the experimenter has complete control, is known as DOE. It entails a group of tests or a sequence of tests in which the input variables of a system or process are purposefully changed. The goal is to methodically monitor and pinpoint the reasons for variations in the output responses [28].

### 2.2.2. RSM

RSM comprises a range of statistical and mathematical techniques that are helpful in modeling and analyzing situations where multiple variables influence an output or response. The objective of RSM is to determine the correlation between the output responses and the input variables.

## 3. Experimental methodology

A full factorial experiment was designed with the following objectives in mind:

- (1) The experimental objectives were established:
  - (a) Minimization of T<sub>m</sub>.
  - (b) Maximization of MRR.
  - (c) Minimization of EWR.
  - (d) Minimization of Ra.
  - (e) Minimization of difference in base radius (R).
- (2) The output (response) variables are selected: T<sub>m</sub>, MRR, EWR, Ra, and R.
- (3) The input (factor) variables are selected: HV, LV, T<sub>on</sub>, and T<sub>off</sub>.

As mentioned in Figure 1, the power curve and factorial design indicates that 2 replicates will give us a 99.95% of detecting significant effects. As a matter of accuracy, we have taken 3 replicates, due to which the number of experiments has reached  $16 \times 3 = 48$ .

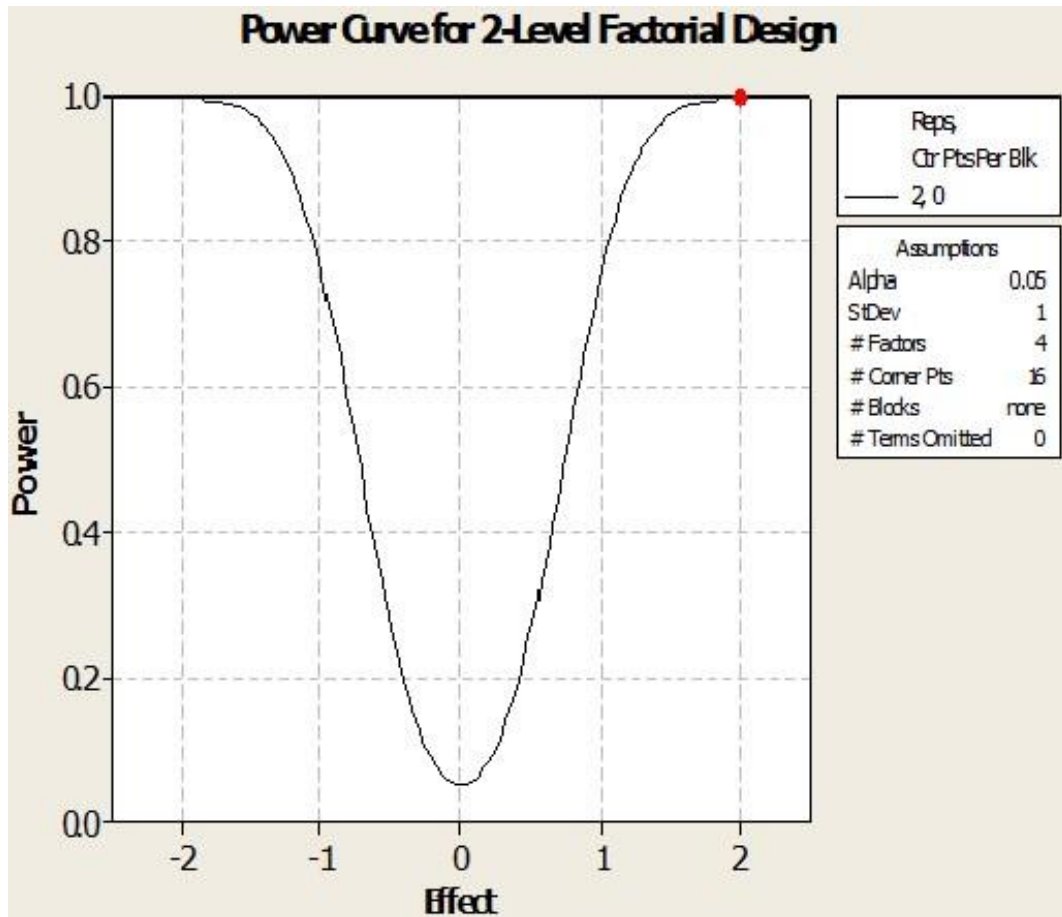


**Figure 1.** Power curve for a 2-level factorial design with 4 factors.

The levels for the input variables were selected and are indicated below in Table 3.

**Table 3.** Factors and their levels.

Factor	Unit	Levels	No. of levels
Workpiece material	-	Ti6Al4V	1
T <sub>on</sub>	μs	4, 6.5	2
T <sub>off</sub>	μs	5.5, 6.5	2
HV	Volts	30, 50	2
LV	Ampere	0.3, 0.7	2

We considered a full factorial design for this research. General notation of the full factorial experiment [29] is mentioned below.

$$2^k = 2^4 = 16 \text{ runs}$$

The power curve and factorial design indicates that 2 replicates will give us a 99.95% of detecting significant effects. As a matter of accuracy, we have taken 3 replicates, due to which the number of experiments has reached  $16 \times 3 = 48$ .

Basic experimental runs are mentioned in Table 4.

**Table 4.** Basic experimental runs.

Run	HV	LV	T <sub>on</sub>	T <sub>off</sub>
1	0.3	30	4	5.5
2	0.7	30	4	5.5
3	0.3	50	4	5.5
4	0.7	50	4	5.5
6	0.7	30	6.5	5.5
7	0.3	50	6.5	5.5
8	0.7	50	6.5	5.5
9	0.3	30	4	6.5
10	0.7	30	4	6.5
11	0.3	50	4	6.5
12	0.7	50	4	6.5
13	0.3	30	6.5	6.5
14	0.7	30	6.5	6.5
15	0.3	50	6.5	6.5
16	0.7	50	6.5	6.5

### 3.1. Workpiece preparation and equipment used

The samples of all workpieces used in these experiments were two grounded blocks of 100 × 10 × 20 mm which were fixed by dwell pins. The electrodes were prepared in a step turned manner with flat circular tip. The diameter of the tip was 3 mm.

A Genspark EDM (PZ type) E5B1041 machine was used to produce 5 mm depth of cut (doc) holes on the workpiece materials for conducting the electrical discharge machining process in hole making. The NC program was fed in the system via the control panel. The T<sub>m</sub> was generated automatically in the system for each experimental run. A surface roughness tester (CONTOURMATIC T2) was used to test surface roughness. A physical balance was used (Scitex, model no. BA-E3121HTP). A stereo microscope was used to observe the workpiece at a 22× magnification level, while the electrode was observed at a 17× magnification to observe wear and material removal pattern.

Electrode wear rate was calculated using the equation [30] mentioned below:

$$EWR = \frac{Eb - Ea}{Tm} \text{ (g/min)}$$

Material removal rate was calculated using the equation [31] mentioned below:

$$MRR = \frac{Wb - Wa}{Tm} \text{ (g/min)}$$

### 3.2. Regression model for Ti6Al4V

A regression model for Ti6Al4V was prepared in Minitab 15 in order to provide a quantitative framework to identify relationships between input factors and output responses, estimate parameters, and validate findings in order to improve experimental results. To visually evaluate the relationships between variables, a matrix plot was first created. Sporadic patterns were preferred, as they are especially relevant to Ti6Al4V.



Every predictor was listed, and metrics like  $R^2$ , adjusted  $R^2$ , Mallows's Cp, and S were assessed, and the total number of predictors was part of the ensuing best subsets analysis.  $R^2$  is the statistical measure known as the coefficient of determination. It evaluates the percentage of the variance in the response output that can be accounted for by the input factors. In other words, it measures the model's goodness of fit. Adjusted  $R^2$  is the modified version of  $R^2$ . Adjusted  $R^2$  adjusts this measure to account for the number of predictors in the model. Its value should be high for better fit of the model. Mallows's Cp weighs the tradeoff between model accuracy and simplicity. The S value was also calculated to check the variability in output responses. Its value should be low for a better fit of the model [32].

Ti6Al4V specific significant predictors were identified by comparing the lowest Mallows's Cp, lowest S, and highest adjusted R-squared as the ideal combination. To establish the baseline equation for Ti6Al4V and confirm significance, the first regression model was run with all factors included. After that, p-values were analyzed at a 95% confidence interval, and factors with values less than 0.05 were considered significant for Ti6Al4V. Furthermore, the variance inflation factor (VIF) was employed to identify any correlation between the predictors. Values falling between 5 and 10 were considered to be poorly estimated coefficients that are specific to the properties of Ti6Al4V. The last regression model was carefully constructed by removing non-significant components, and the resulting formula was assessed, paying particular attention to the adjusted R-squared value to take the particular number of predictors in the Ti6Al4V model into consideration. This methodical process guarantees the creation of a reliable and customized regression model for Ti6Al4V.

The final regression equation was evaluated, and the R-Sq (adj) [33] value was taken, which accounts for number of predictors in the model.

$$R - Sq(adj) = \frac{SS_{Regression} - MS_{Error}}{SS_{Total}}$$

## 4. Results and discussion

### 4.1. Experimental results and analysis

#### 4.1.1. Statistical analysis of experimental results

As a critical statistical tool for adjusting parameters in the electrical discharge machining procedure especially designed for Ti6Al4V, the application of analysis of variance (ANOVA) assumes a central role [7]. The statistical significance of mean variations resulting from various parameter settings can be thoroughly examined through the application of ANOVA. In addition to providing insights into the ideal parameter combination for increased efficiency and precision in the machining process, this analysis also forms a crucial basis for comprehending and identifying the major factors that significantly impact the EDM outcomes for Ti6Al4V.

The statistical analysis of experimental results was conducted, and ANOVA was performed in Minitab 15. Detailed ANOVA pictures are presented in Appendix 3. Pictures of workpiece Ti6Al4V and copper electrode at different input settings are present in Appendix 5. A summary of results is given below.

#### 4.1.1.1. $T_m$ optimized results

The ANOVA was performed for  $T_m$  in Minitab, and its complete details are presented in Appendix 3. The ANOVA table in Table A3 and the normal probability plot in Figure A4 indicate that LV and  $T_{on}$  are significant factors when considering  $T_m$  for Ti6Al4V. The p-values from the ANOVA Table A4 of the refitted model indicate that the models as well as these factors are significant. After developing the ANOVA tables for significant factors, the main effects plot in Figure A8 and the interaction plot in Figure A9 were prepared. The main effects plot shows a steep slope of means, indicating the significance of LV and  $T_{on}$ . The interaction plot shows non-parallel lines of significance. Next, the optimized values of significant factors are to be calculated. For optimization of machining time, we have set the target value to 0 and the upper value to 1375, which is the maximum value of machining time, and then the values of desirability functions are evaluated.

$d = 0$  emphasizes that  $y$  or response is more away from the target because the target was taken as “0” and response comes out to be far away from upper value that was taken as 1375. It could have been  $d = 1$  or close to 1, if the target was set close to 1500, and the upper value was taken as greater than, say, 2200. The optimized value for LV is 50 A, while for  $T_{on}$  it is 6.5  $\mu$ s, as mentioned in Appendix 1. For these values, maximum  $T_m$  is 2069.5417 seconds.

It can be seen from the results in Appendix 1 that when LV and  $T_{on}$  values are higher, resultant  $T_m$  was less as compared to other values when LV and  $T_{on}$ . In EDM, LV and  $T_{on}$  are inversely proportional to each other, as can be observed from experimental runs mentioned in Appendix 1. But higher LV and  $T_{on}$  time values lead to larger craters on the workpiece which ultimately impact the surface finish ( $R_a$ ) of the product. That is why the parametric optimization of the EDM was carried to strike a balance between all the output responses in order to get an excellent final product.

#### 4.1.1.2. MRR optimized results

The ANOVA table presented as Table A5 of Appendix 3 and the normal probability plot in Figure A11 indicate that LV and  $T_{on}$  are significant factors while considering MRR for Ti6Al4V. The p-values from the ANOVA Table A6 of the refitted model indicate that the models as well as these factors are significant. After developing the ANOVA tables for significant factors, the main effects plot in Figure A15 and the interaction plot in Figure A16 were prepared for MRR. The interaction plot shows non-parallel lines of significance in Figure A16. Next, the optimized values of significant factors are to be calculated. For optimization of material removal rate, we have set the target value to 1 and the lower value to 0.00291 g/min, which is the maximum value of material removal rate. Then, the values of desirability functions were evaluated.

$d = 0$  emphasizes that  $y$  response is more away from the target because the target was taken as “1” and response comes out to be far away from the lower value that was taken as 0.00291. It could have been  $d = 1$  or close to 1, if the target was set close to 0.002 and the lower value was taken as less than, say, 0.001. The optimized value for LV is 50 A, while for  $T_{on}$  it is 6.5  $\mu$ s. For these values, maximum MRR is 0.0022 g/min.

LV and  $T_{on}$  are directly proportional to MRR, as can be seen in Appendix 1. For the same value of  $T_{on}$ , higher values of LV have greater MRR. However, higher values of current will lead to larger craters on the workpiece, leading to poor surface finish. Parametric optimization was performed for MRR in order to resolve this issue.

#### 4.1.1.3. EWR optimized results

The ANOVA Table A7 in Appendix 3 for EWR was prepared in Minitab considering all factors, and then the significant factors were determined as having p-values less than 0.05. The goal in mind was minimization of electrode wear rate. The ANOVA table presented as Table A7 of Appendix 3 and the normal probability plot in Figure A18 indicate that LV is a significant factor when considering EWR for Ti6Al4V. After that, the model was refitted by eliminating the non-significant values and considering only LV as an input factor. The p-values from the ANOVA of the refitted model (Table A8) indicate that the models as well as these factors are significant. After developing the ANOVA tables for significant factors, the main effects plot (Figure A22) and the interaction plot (Figure A23) were prepared for EWR. The main effects plot shows a steep slope of means, indicating the significance of these factors. The interaction plot shows non-parallel lines of significance. Next, the optimized values of significant factors were calculated. For optimization of material removal rate, we have set the target value to 0 and the upper value to 0.00304 g/min, which is the minimum value of electrode wear rate, and then the values of desirability functions were evaluated.

$d = 0.00252$  emphasizes that response is more away from the target because the target was taken as “1” and response comes out to be far away from the upper value that was taken as 0.00304. It could have been  $d = 1$  or close to 1, if the target was set close to 0.004 and the upper value was taken as greater than, say, 0.006. The optimized value for LV is 30 A, for which value the minimum EWR is 0.0055 g/min.

EWR is directly proportional to LV as current directly influences the intensity of electrical discharges and consequently leads to erosion of electrode material. As can be seen in Appendix 1, higher LV values have greater EWR due to more aggressive MRR in each discharge cycle. This occurs because of higher currents leading to greater energy densities at the electrode-workpiece interface, causing more rapid erosion of electrode material [34].

#### 4.1.1.4. Ra optimized results

The ANOVA table in Table A9 for Ra was prepared in Minitab and is presented in Appendix 3 considering all factors, and the significant factors were determined as having p-values less than 0.05. The goal in mind was minimization of surface roughness.

The ANOVA table presented as Table A9 of Appendix 3 and the normal probability plot in Figure A29 indicate that  $T_{\text{off}}$  and the interaction of  $HV*LV*T_{\text{off}}$  are significant factors when considering Ra for Ti6Al4V. The model was refitted by eliminating the non-significant values and considering only  $T_{\text{off}}$  and  $HV*LV*T_{\text{off}}$  as input factors. The p-values from the ANOVA of the refitted model (Table A10) indicate that the models as well as these factors are significant. After developing the ANOVA tables for significant factors, the main effects plot (Figure A29) and the interaction plot (Figure A30) were prepared for Ra. The main effects plot shows a steep slope of means, indicating the significance of these factors. The interaction plot shows non-parallel lines of significance. Next, the optimized values of significant factors were calculated. For optimization of surface roughness, we set the target value to 0 and the upper value to 0.007, which is the minimum value of surface roughness. Then, the values of the desirability functions were evaluated.

$d = 0$  emphasizes that response is more away from the target because the target was taken as “0” and response comes out to be far away from the upper value that was taken as 0.007. It could have

been  $d = 1$  or close to 1, if the target was set close to 0.01 and the upper value was taken as greater than, say, 0.03. The optimized value for HV is 0.70 V, LV is 30 A, and  $T_{\text{off}}$  is 6.5  $\mu\text{s}$ . For these values, minimum Ra is 0.009 mm.

LV and surface finish (Ra) are directly proportional to each other. Higher current leads to increased MRR but also results in higher values of Ra. As can be seen in the experimental runs in Appendix 1, higher current leads to higher values of Ra.

Voltage plays a significant role in determining the surface finishes of the workpiece. Higher voltages generate more energetic discharges which result in lower values of Ra, as can be seen in Appendix 1.

#### 4.1.1.5. Base radius (R) optimized results

The ANOVA table in Table A11 for R was prepared in Minitab considering all factors, and then the significant factors were determined as having p-values less than 0.05. The goal in mind was optimization of base radius.

The ANOVA table for base radius presented in Appendix 3 as Table A11 and the normal probability plot in Figure A32 indicate that  $T_{\text{on}}$  is a significant factor when considering R for Ti6Al4V. The model was refitted by eliminating the non-significant values and considering only  $T_{\text{on}}$  as an input factor. The p-values from the ANOVA of the refitted model (Table A12) indicate that the models as well as these factors are significant. After developing the ANOVA tables for significant factors, the main effects plot (Figure A36) and the interaction plot (Figure A37) were prepared for R. The main effects plot shows a steep slope of means, indicating the significance of these factors. The interaction plot shows near parallel lines of non-significance between  $T_{\text{on}}$  and LV. Next, the optimized values of significant factors were calculated. For optimization of base radius value, we set the target value to 1.5 and the upper and lower values to 1.55 and 1.45, respectively. Then, the values of the desirability functions were evaluated. The specific desirability function ( $d$ ) equals to 1 and it means that desirability for a response increases linearly. The optimized value for  $T_{\text{on}}$  is 5.8003 for the optimized R value of 1.5 mm.

In this research study, the focus was on the parametric optimization of all output responses pertaining to Ti6Al4V within a controlled environment. Also, emphasis was on the fabrication of delicate and small components, particularly tailored for intricate biomedical applications such as tooth implants or bone support. The imperative criteria for these applications included the simultaneous achievement of both strength and fine details.

To address this, input factors were set at low settings. Five distinct output responses were optimized simultaneously, which is a unique approach in the context of Ti6Al4V. Notably, previous research efforts, demonstrated by studies such as [25,35], predominantly concentrated on the optimization of only one or two output responses at a time.

#### 4.1.2. Regression analysis results

Regression analysis for Ti6Al4V was carried out for all responses for which details are presented. The following are the results of the regression.

**Regression for Tm on Ti6Al4V:** The regression analysis indicates that there is no significant factor when Tm is considered for Ti6Al4V.

**Regression for MRR on Ti6Al4V:** The regression equation is

$$\text{MRR} = 0.000013 + 0.000003 \cdot T_{\text{on}}$$

The regression equation shows a positive sign prior to  $T_{\text{on}}$ , which means that the higher  $T_{\text{on}}$  is, the higher the MRR will be. Also, as a result of regression analysis,  $T_{\text{on}}$  is the significant predictor for MRR.

**Regression for EWR on Ti6Al4V:** The regression analysis indicates that there is no significant factor when EWR is considered for Ti6Al4V.

**Regression for Ra on Ti6Al4V:** The regression analysis indicates that there is no significant factor when Ra is considered for Ti6Al4V.

**Regression for R on Ti6Al4V:** The regression analysis indicates that there is no significant factor when R is considered for Ti6Al4V.

## 5. Conclusions

In conclusion, this research study concentrated on the use of EDM, specifically on Ti6Al4V machining. The primary objective of this paper was to conduct a comprehensive optimization of five critical output responses ( $T_m$ , MRR, EWR, Ra, R) while operating at extremely low settings of input factors (HV, LV,  $T_{\text{on}}$ ,  $T_{\text{off}}$ ). The significance of this study lies in its departure from the conventional norm, as most research endeavors in this domain typically focus on optimizing one or two responses at a time. Through a single experiment, we successfully identified the key input factors through regression to exert a substantial influence on the targeted output responses. Key findings of this investigative study are as follows.

It can be seen in the pictures of the workpieces at different input settings in Appendix 5 that high discharge energy causes deeper and larger craters, reducing the surface finish. Reducing the current intensity resulted in less damage and improved surface quality. The highest MRR was achieved with a combination of high discharge current (LV = 50 A) and pulse time ( $T_{\text{on}} = 6.5 \mu\text{s}$ ), while the lowest MRR was seen at the lowest range of machining variables. MRR increases with discharge current and pulse on time, whereas voltage and pulse off time have no significant effect.

The minimum value of Ra was achieved under these input parameters: HV is 0.70 V, LV is 30 A, and  $T_{\text{off}}$  is  $6.5 \mu\text{s}$ . LV and Ra are directly proportional to each other. Higher current leads to increased MRR but also results in higher values of Ra. Higher current leads to higher values of Ra. Voltage plays a significant role in determining the surface finishes of the workpiece. Higher voltages generate more energetic discharges which result in lower values of Ra.

The minimum value of machining time was observed with the parameters LV = 50 A and  $T_{\text{on}} = 6.5 \mu\text{s}$ . When LV and  $T_{\text{on}}$  values are higher, the  $T_m$  reduced. In EDM, LV and  $T_{\text{on}}$  are inversely proportional to each other, as can be observed from the experimental runs presented in Appendix 1.

The optimized value of EWR was achieved at LV = 30, which was the lowest value of current settings. EWR is directly proportional to LV, as current directly influences the intensity of electrical discharges and consequently leads to erosion of electrode material.

This unique approach to optimizing multiple responses concurrently, under controlled settings, holds immense potential for industries engaged in the production of products utilizing Ti6Al4V material, particularly in the realm of biomedical implants such as tooth implants and bone supports. While Ti6Al4V implants are renowned for their exceptional strength, their manufacturing has posed challenges with traditional methods.

Achieved objectives and their implications are as follows:

**Machining Time Reduction:**

LV and pulse on time are significant factors influencing the reduction of machining time for Ti6Al4V.

Optimized values: LV = 50 A, pulse on time = 6.5  $\mu$ s.

Achieved minimum machining time: 2069.5417 seconds.

**Material Removal Rate Maximization:**

LV and pulse on time play crucial roles in maximizing material removal rate for Ti6Al4V.

Optimized values: LV = 50 A, pulse on time = 6.5  $\mu$ s.

Achieved maximum material removal rate: 0.0022 g/min.

**Electrode Wear Rate Minimization:**

LV is a significant factor in minimizing electrode wear rate for Ti6Al4V.

Optimized value: LV = 30 A.

Achieved minimum electrode wear rate: 0.0055 g/min, compared to a previous study [36] with an optimized EWR of 0.10 mm<sup>3</sup>/min.

**Surface Roughness Minimization:**

Pulse off time and the interaction HV\*LV\*T<sub>off</sub> significantly impact surface roughness minimization for Ti6Al4V.

Optimized values: HV = 0.70 V, LV = 30 A, pulse off time = 6.5  $\mu$ s.

Achieved minimum Ra (average roughness): 0.009 mm.

**Base Radius Dimensions:**

Pulse on time is the significant factor affecting base radius dimensions for Ti6Al4V.

Optimized value: pulse on time = 5.8003  $\mu$ s.

Achieved optimized base radius: 1.5 mm.

The optimized output responses achieved in this study, executed at reduced settings, carry far-reaching implications. Specifically, the potential benefits extend to industries striving for high production efficiency and cost-effectiveness. Tooth implants, when produced with Ti6Al4V material under the optimized parameters, promise enhanced units per hour (UPH) with superior surface finishes. The optimization of T<sub>m</sub> not only maximizes production units per hour but also contributes to operational cost reduction through the careful use of materials and electricity.

The implications of this research extend beyond mere efficiency gains. The attainment of excellent surface finishes is poised to yield end products of superior quality, free from issues such as burrs. Moreover, the optimization strategy employed in minimizing the EWR translates to reduced material usage and fewer change-ups, thereby amplifying production UPH and concurrently diminishing material costs.

In essence, this study not only contributes valuable insights to the field of Ti6Al4V machining but also offers tangible solutions for industries aiming to enhance productivity, reduce operational costs, and deliver high-quality biomedical implants to end-users.

This research pertains to United Nations Sustainable Development Goal 12, focusing on “Responsible Consumption and Production” (Figure 2).

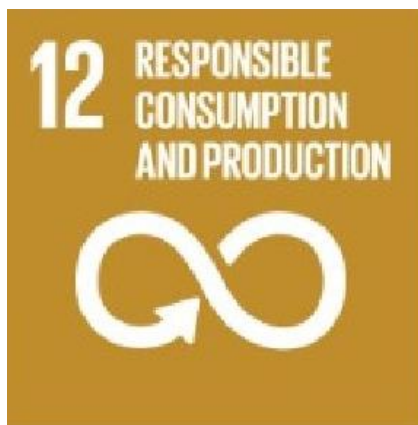


**Figure 2.** Responsible consumption and production—SDG’s.

### Use of AI tools declaration

The authors declare they have not used artificial intelligence (AI) tools in the creation of this article.

### Author contributions

All authors contributed to the study, idea conception, and design. Material preparation, data collection, and analysis were performed by Muhammad Mansoor uz Zaman Siddiqui, Prof. Dr. Syed Amir Iqbal, Ali Zulqarnain, and Adeel Tabassum. The first draft of the manuscript was written by Muhammad Mansoor uz Zaman Siddiqui, and all authors commented on previous versions of the manuscript. All authors read and approved the final manuscript.

### Conflict of interest

The authors declare no conflict of interest.

### References

1. Okokpujie IP, Bolu CA, Ohunakin OS, et al. (2019) A review of recent application of machining techniques, based on the phenomena of CNC machining operations. *Procedia Manuf* 35: 1054–1060. <https://doi.org/10.1016/j.promfg.2019.06.056>
2. Natsu W, He J, Iwanaga Y (2020) Experimental study on electrochemical machining with electrolyte confined by absorption material. *Procedia CIRP* 87: 263–267. <https://doi.org/10.1016/j.procir.2020.02.106>
3. Farooq MU, Anwar S, Bhatti HA, et al. (2023) Electric discharge machining of Ti6Al4V ELI in biomedical industry: Parametric analysis of surface functionalization and tribological characterization. *Materials* 16: 4458. <https://doi.org/10.3390/ma16124458>
4. Happonen A, Stepanov A, Piili H, et al. (2015) Innovation study for laser cutting of complex geometries with paper materials. *Phys Procedia* 78: 128–137. <https://doi.org/10.1016/j.phpro.2015.11.025>

5. Gilmore R (1991) Ultrasonic machining: A case study. *J Mater Process Tech* 28: 139–148. [https://doi.org/10.1016/0924-0136\(91\)90213-X](https://doi.org/10.1016/0924-0136(91)90213-X)
6. Samsudeensadham S, Mohan A, Krishnaraj V (2021) A research on machining parameters during dry machining of Ti-6Al-4V alloy. *Mater Today: Proc* 46: 9354–9360. <https://doi.org/10.1016/j.matpr.2020.02.821>
7. Prasad AVSR, Ramji K, Datta GL (2014) An experimental study of wire EDM on Ti-6Al-4V alloy. *Procedia Mater Sci* 5: 2567–2576. <https://doi.org/10.1016/j.mspro.2014.07.517>
8. Rathod R, Kamble D, Ambhore N (2022) Performance evaluation of electric discharge machining of titanium alloy—A review. *J Eng Appl Sci* 69: 64. <https://doi.org/10.1186/s44147-022-00118-z>
9. Nagadeepan A, Jayaprakash G, Senthilkumar V (2023) Advanced optimization of surface characteristics and material removal rate for biocompatible Ti6Al4V using WEDM process with BBD and NSGA II. *Materials* 16: 4915. <https://doi.org/10.3390/ma16144915>
10. Dewangan S, Kumar SD, Jha SK, et al. (2020) Optimization of micro-EDM drilling parameters of Ti-6Al-4V alloy. *Mater Today: Proc* 33: 5481–5485. <https://doi.org/10.1016/j.matpr.2020.03.307>
11. Garba E, Abdul-Rani AM, Yunus NA, et al. (2023) A review of electrode manufacturing methods for electrical discharge machining: Current status and future perspectives for surface alloying. *Machines* 11: 906. <https://doi.org/10.3390/machines11090906>
12. Banu A, Ali MY (2016) Electrical discharge machining (EDM): A review. *Int J Eng Mater Manuf* 1: 3–10. <https://doi.org/10.26776/ijemm.01.01.2016.02>
13. Galati M, Antonioni P, Calignano F, et al. (2023) Experimental investigation on the cutting of additively manufactured Ti6Al4V with wire-EDM and the analytical modelling of cutting speed and surface roughness. *J Manuf Mater Process* 7: 69. <https://doi.org/10.3390/jmmp7020069>
14. Kamenskikh AA, Muratov KR, Shlykov ES, et al. (2023) Recent trends and developments in the electrical discharge machining industry: A review. *J Manuf Mater Process* 7: 204. <https://doi.org/10.3390/jmmp7060204>
15. Ram JS, Jeavudeen S, Mouda PA, et al. (2023) The role of various dielectrics used in EDM process and their environmental, health, and safety issues. *Mater Today: Proc.* <https://doi.org/10.1016/j.matpr.2023.05.137>
16. Nadda R, Nirala CK, Singh PK, et al. (2024) An overview of techniques for monitoring and compensating tool wear in micro-electrical discharge machining. *Heliyon* 10: e26784. <https://doi.org/10.1016/j.heliyon.2024.e26784>
17. Nguyen VQ, Duong TH, Kim HC (2015) Precision micro EDM based on real-time monitoring and electrode wear compensation. *Int J Adv Manuf Tech* 79: 1829–1838. <https://doi.org/10.1007/s00170-015-6964-y>
18. Di Campli R, Maradia U, Boccadoro M, et al. (2020) Real-time wire EDM tool simulation enabled by discharge location tracker. *Procedia CIRP* 95: 308–312. <https://doi.org/10.1016/j.procir.2020.01.176>
19. Mhatre MS, Sapkal SU, Pawade RS (2014) Electro discharge machining characteristics of Ti-6Al-4V alloy: A grey relational optimization. *Procedia Mater Sci* 5: 2014–2022. <https://doi.org/10.1016/j.mspro.2014.07.534>
20. Gu L, Li L, Zhao W, et al. (2012) Electrical discharge machining of Ti6Al4V with a bundled electrode. *Int J Mach Tool Manu* 53: 100–106. <https://doi.org/10.1016/j.ijmactools.2011.10.002>



21. Świercz R, Oniszczyk-Świercz D, Chmielewski T (2019) Multi-response optimization of electrical discharge machining using the desirability function. *Micromachines* 10: 72. <https://doi.org/10.3390/mi10010072>
22. Maniyar KG, Ingole DS (2018) Multi response optimization of EDM process parameters for aluminium hybrid composites by GRA. *Mater Today: Proc* 5: 19836–19843. <https://doi.org/10.1016/j.matpr.2018.06.347>
23. Agarwal N, Irshad M, Singh M R, et al. (2022) Optimization of material removal rate of Ti-6Al-4V using Rao-1 algorithm. *Mater Today: Proc* 62: 6722–6726. <https://doi.org/10.1016/j.matpr.2022.04.760>
24. Klocke F, Schwade M, Klink A, et al. (2013) Analysis of material removal rate and electrode wear in sinking EDM roughing strategies using different graphite grades. *Procedia CIRP* 6: 163–167. <https://doi.org/10.1016/j.procir.2013.03.079>
25. Kumar R, Roy S, Gunjan P, et al. (2018) Analysis of MRR and surface roughness in machining Ti-6Al-4V ELI titanium alloy using EDM process. *Procedia Manuf* 20: 358–364. <https://doi.org/10.1016/j.promfg.2018.02.052>
26. Shao F, Liu Z, Wan Y, et al. (2010) Finite element simulation of machining of Ti-6Al-4V alloy with thermodynamical constitutive equation. *Int J Adv Manuf Tech* 49: 431–439. <https://doi.org/10.1007/s00170-009-2423-y>
27. Caballero B, Finglas P, Toldrá F (2016) *Encyclopedia of Food and Health*, New York: Academic Press, 321–326.
28. Iqbal A, Khan AA (2010) Modeling and analysis of MRR, EWR and surface roughness in EDM milling through response surface methodology. *Am J Eng Appl Sci* 3: 611–619. <https://doi.org/10.3923/jeasci.2010.154.162>
29. Liu Y, Fearn T, Strlič M (2021) Factorial experimentation on photodegradation of historical paper by polychromatic visible radiation. *Herit Sci* 9: 130. <https://doi.org/10.1186/s40494-021-00602-4>
30. Sultan T, Kumar A, Gupta RD (2014) Material removal rate, electrode wear rate, and surface roughness evaluation in die sinking EDM with hollow tool through response surface methodology. *Int J Manuf Eng* 2014: 259129. <https://doi.org/10.1155/2014/259129>
31. Seshaiyah S, Sampathkumar D, Mariappan M, et al. (2022) Optimization on material removal rate and surface roughness of stainless steel 304 wire cut EDM by response surface methodology. *Adv Mater Sci Eng* 2022: 6022550. <https://doi.org/10.1155/2022/6022550>
32. Jin HT, Wang F, Zhang W, et al. (2023) Linear regression analysis of sleep quality in people with insomnia in Wuhan city during the COVID-19 pandemic. *Int J Clin Pract* 2023: 6746045. <https://doi.org/10.1155/2023/6746045>
33. Sarstedt M, Mooi E (2014) *A Concise Guide to Market Research*, 2 Eds., Berlin: Springer, 193–233.
34. Harane PP, Wojciechowski S, Unune DR (2022) Investigating the effect of different tool electrodes in electric discharge drilling of Waspaloy on process responses. *J Mater Res Technol* 20: 2542–2557. <https://doi.org/10.1016/j.jmrt.2022.08.015>
35. Devarajaiah D, Muthumari C (2018) Evaluation of power consumption and MRR in WEDM of Ti-6Al-4V alloy and its simultaneous optimization for sustainable production. *J Braz Soc Mech Sci* 40: 400. <https://doi.org/10.1007/s40430-018-1318-y>
36. Tang L, Du YT (2014) Experimental study on green electrical discharge machining in tap water of Ti-6Al-4V and parameters optimization. *Int J Adv Manuf Tech* 70: 469–475. <https://doi.org/10.1007/s00170-013-5274-5>



AIMS Press

© 2024 the Author(s), licensee AIMS Press. This is an open access article distributed under the terms of the Creative Commons Attribution License (<https://creativecommons.org/licenses/by/4.0>)